Electronic Supplementary Material (ESI) for Journal of Materials Chemistry B.

Supporting Information for

Simultaneous Sensing of Ferritin and Apoferritin Proteins Using an Iron-Responsive Dye and Evaluation of Physiological Parameters Associated with Serum Iron Estimation

Nilanjan Dey,[a] Asfa Ali,[a] Mohini Kamra [a] and Santanu Bhattacharya*[a,b]

[a]Department of Organic Chemistry, Indian Institute of Science, Bangalore 560 012, India.
[b]Indian Association for Cultivation of Science, Jadavpur, Kolkata 700032, India
Email: sb23in@yahoo.com

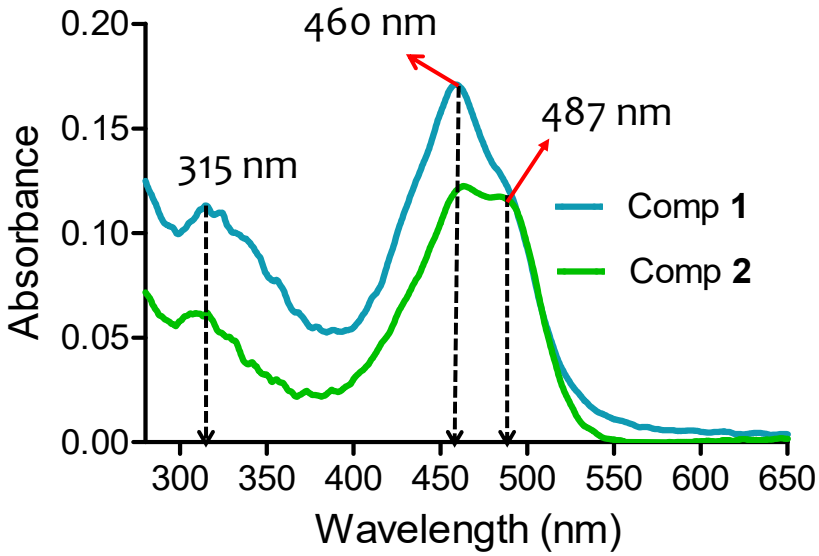

Figure S1. UV-visible spectra of compounds **1** and **2** at pH 7.4 in water.

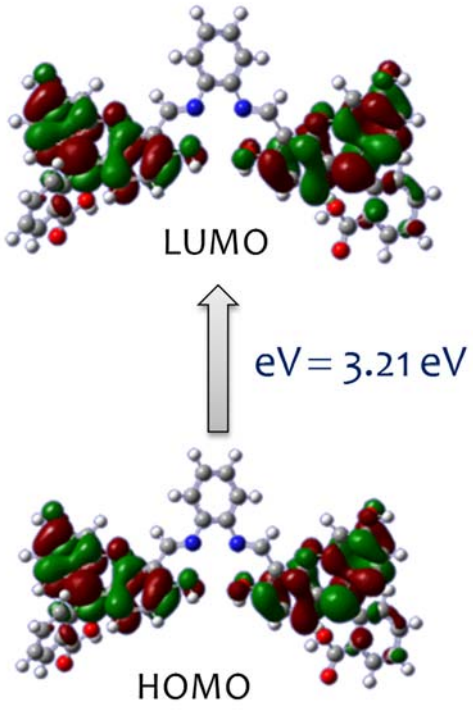

Figure S2. FMO analysis of compound **1** using B3LYP/6-31G* method.

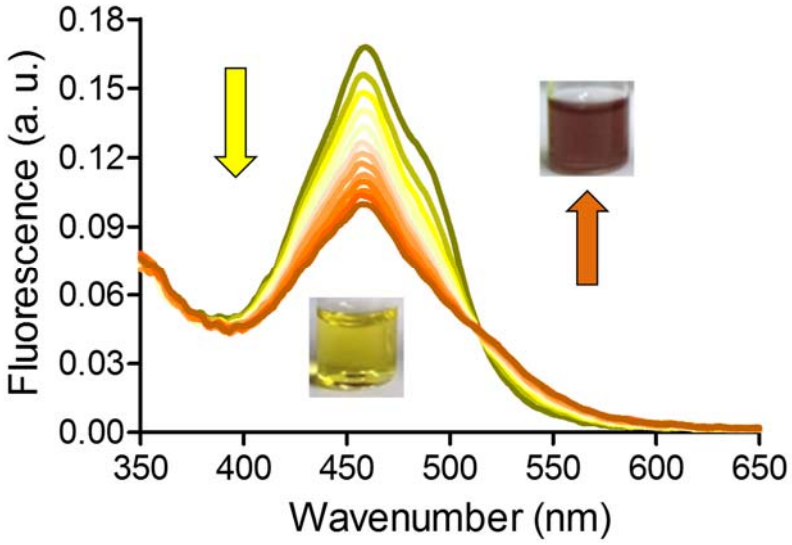

Figure S3. UV-visible titration of **1** (10 μM) with Fe^{2+} (0-10 μM) at pH 7.4 in water

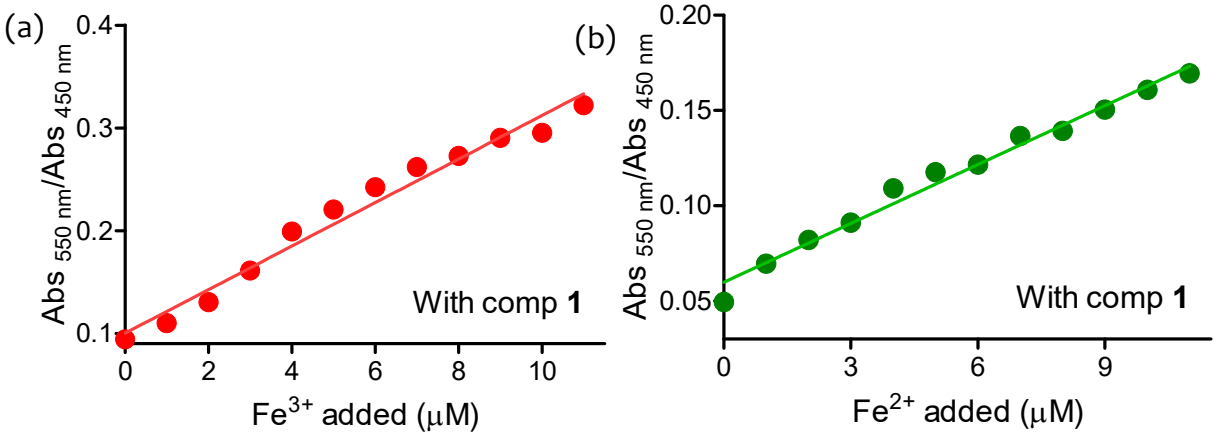

Figure S4. (a) Ratiometric variation in absorbance of **1** (10 μM) during titration with Fe^{3+} (0-10 μM) at pH 7.4 in water; (b) Ratiometric variation in absorbance of **1** (10 μM) during titration with Fe^{2+} (0-10 μM) at pH 7.4 in water.

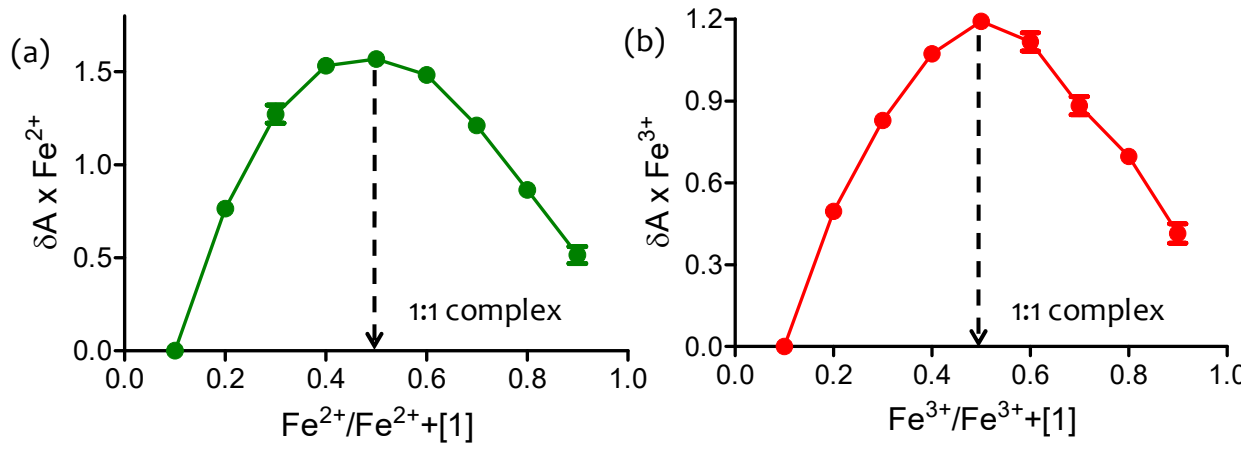

Figure S5. (a) Determination of stoichiometry of interaction of **1** with Fe^{2+} at pH 7.4 in water; (b) Determination of stoichiometry of interaction of **1** with Fe^{2+} at pH 7.4 in water

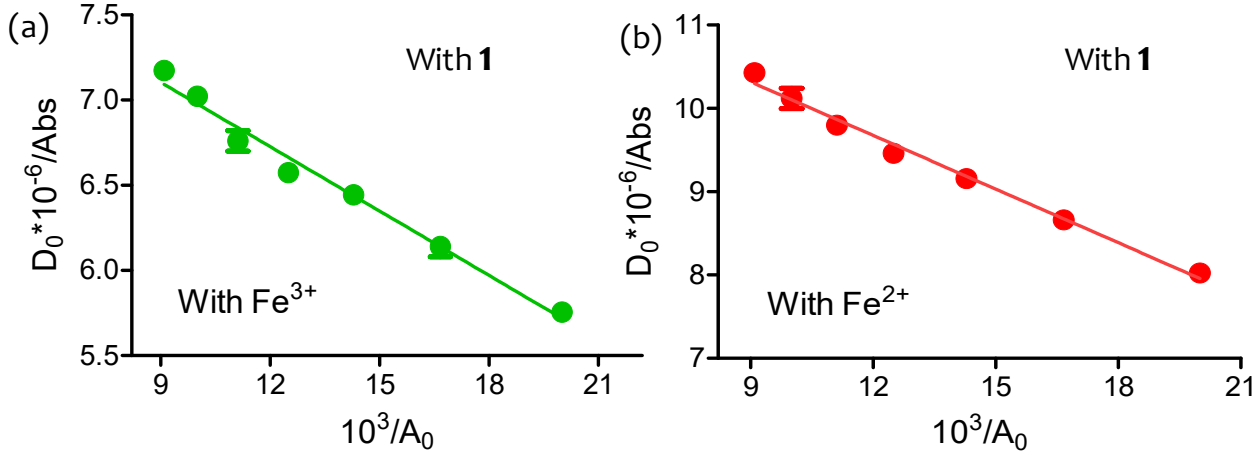

Figure S6. (a) Determination of binding constant of **1** with Fe^{3+} at pH 7.4 in water based on 1:1 binding model; (b) Determination of binding constant of **1** with Fe^{2+} at pH 7.4 in water based on 1:1 binding model

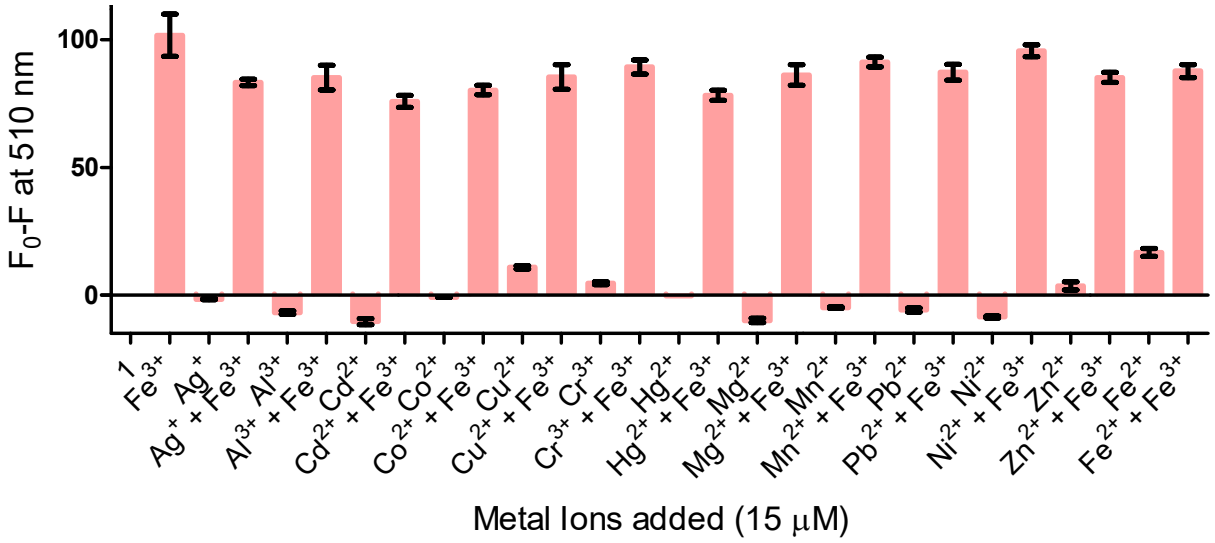

Figure S7. Change in emission intensity of **1** (10 μM, λ_{ex} = 457 nm) at 510 nm upon addition of Fe^{3+} (10 μM) in presence of different metal ions (15 μM) at pH 7.4 in water.

Calculation of Stern-Volmer quenching constant: For collisional quenching, the Stern-Volmer equation is, $F_o/F = 1 + KSV[Fe^{3+}]$ where F_o and F are the fluorescence intensities observed in the absence and presence, respectively, of quencher, $[Fe^{3+}]$ is the quencher concentration and K_{SV} is the Stern-Volmer quenching constant. Thus, a plot of F_o/F versus $[Fe^{3+}]$ should yield a straight line with a slope equal to K_{SV}.

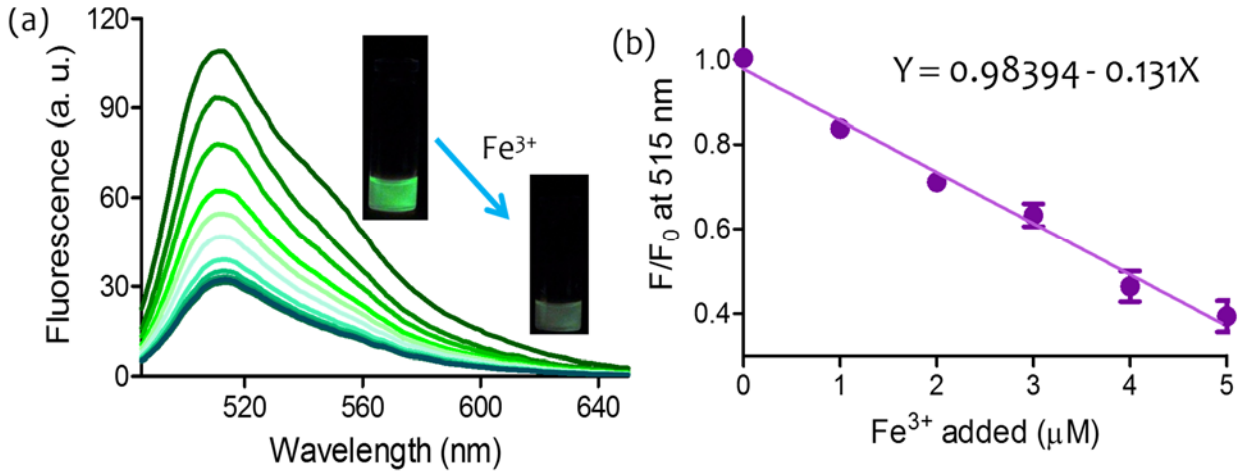

Figure S8. (a) Fluorescence titration of **1** (10 μM, λ_{ex} = 457 nm) with Fe^{3+} (0-10 μM) at pH 7.4 in water. (b) Change in emission intensity of **1** (10 μM, λ_{ex} = 457 nm) at 515 nm upon addition of Fe^{3+} (0-10 μM) at pH 7.4 in water.

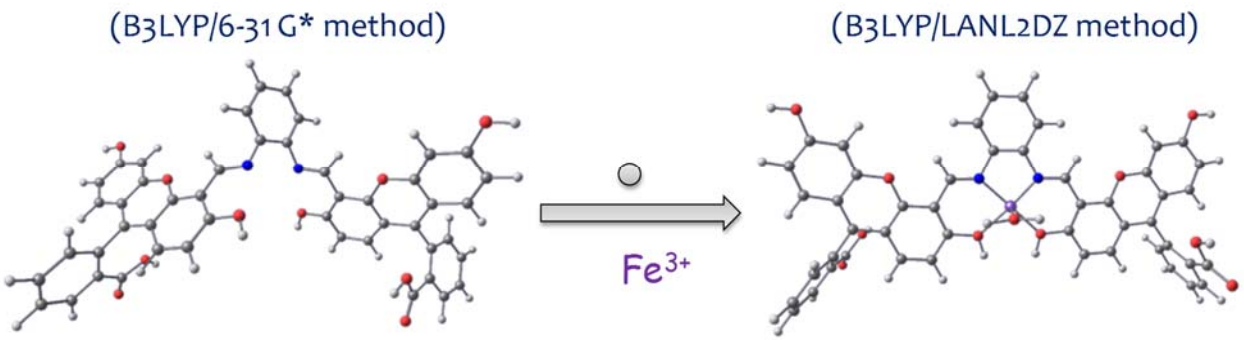

Figure S9. Energy minimized structures of compound **1** and **1**+Fe^{3+} using B3LYP/6-31G* level of theory (LANL2DZ for Fe).

System	Müllikan charge	Dihedral angles	Binding energy (eV)	HOMO-LUMO gap (eV)	Internal energy (a. u.)
1	O1: -0.432 O2: -0.428 N1: -0.596 N2: -0.554	< N-C-C-O = 10.28°	-	3.21 eV (f = 0.0718)	-2678.29
1 + Fe^{3+}	O1: -0.230 O2: -0.278 N1: -0.331 N2: -0.305	< N-C-C-O = 0.08°	3.71 eV	1.54 eV (f = 0.1030)	-2831.15

Table S1. Structural parameters of **1** and **1**+Fe^{3+} using B3LYP/6-31G* level of theory (LANL2DZ for Fe)

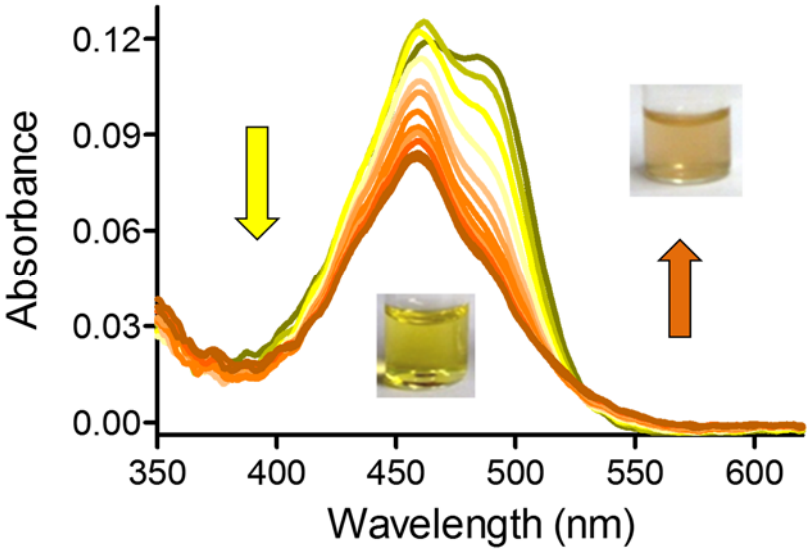

Figure S10. UV-visible titration of **2** (10 μM) with Fe^{2+} (0-10 μM) at pH 7.4 in water

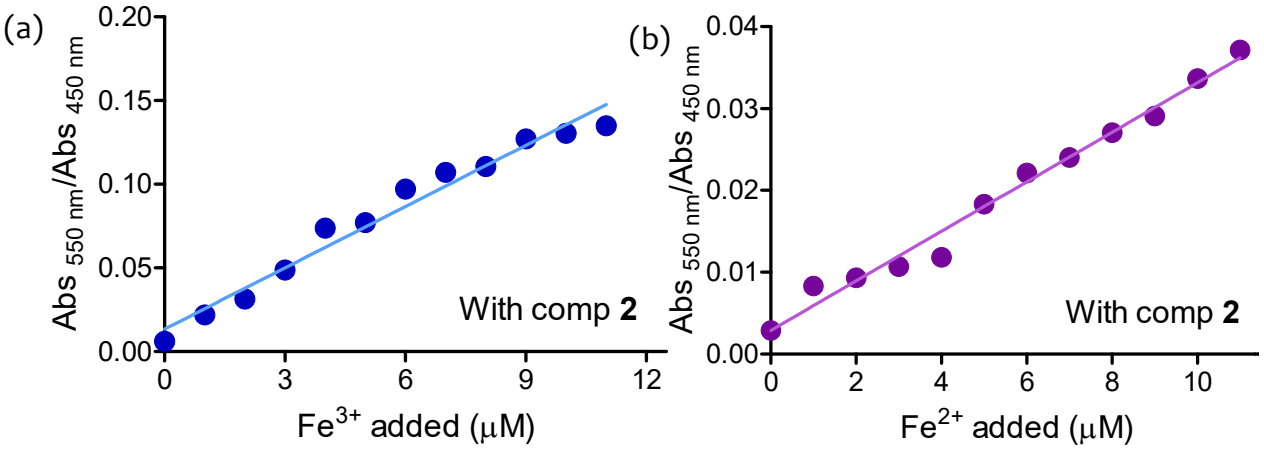

Figure S11. (a) Ratiometric variation in absorbance of **2** (10 μM) during titration with Fe^{3+} (0-10 μM) at pH 7.4 in water; (b) Ratiometric variation in absorbance of **2** (10 μM) during titration with Fe^{2+} (0-10 μM) at pH 7.4 in water

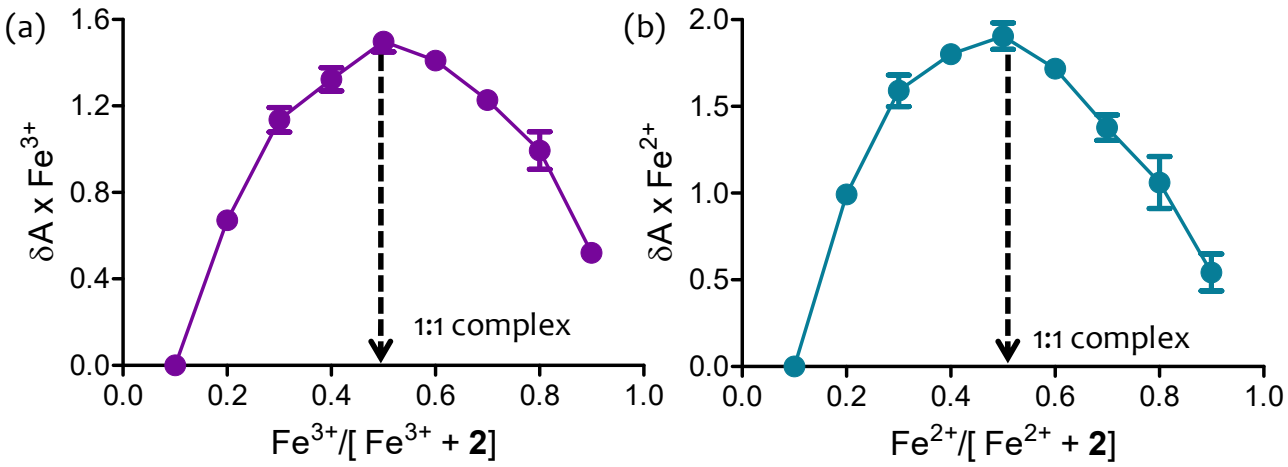

Figure S12. (a) Determination of stoichiometry of interaction of **2** with Fe^{2+} at pH 7.4 in water; (b) Determination of stoichiometry of interaction of **2** with Fe^{2+} at pH 7.4 in water

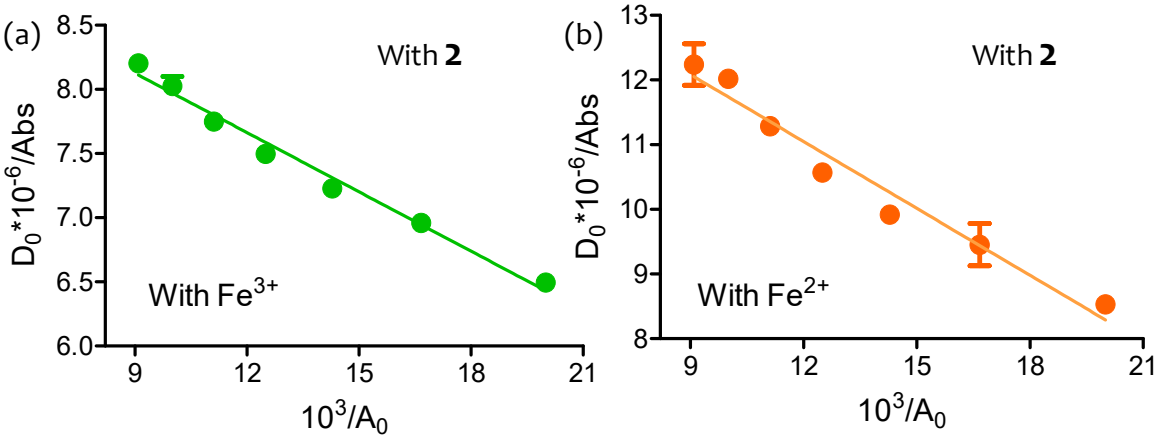

Figure S13. (a) Determination of binding constant of **2** with Fe^{3+} at pH 7.4 in water based on 1:1 binding model; (b) Determination of binding constant of **2** with Fe^{2+} at pH 7.4 in water based on 1:1 binding model

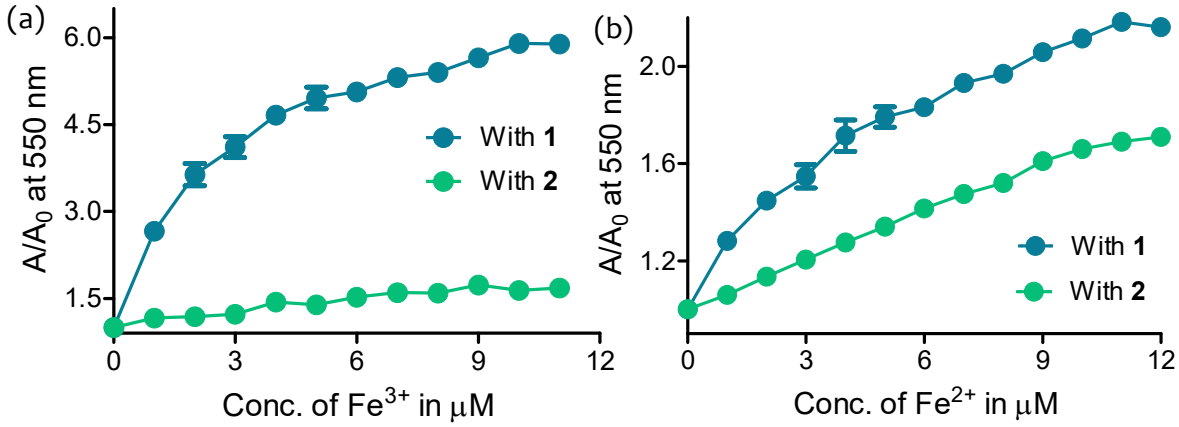

Figure S14. (a) Change in absorbance of **1** and **2** (10 μM) at 550 nm upon addition of Fe^{3+} (0-11 μM) at pH 7.4 in water; (b) Change in absorbance of **1** and **2** (10 μM) at 550 nm upon addition of Fe^{2+} (0-11 μM) at pH 7.4 in water

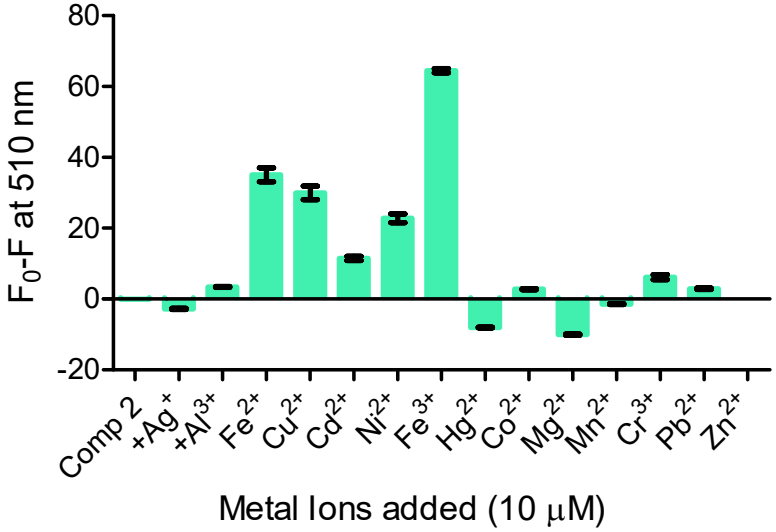

Figure S15. Change in fluorescence of **2** (10 μM, λ_{ex} = 457 nm) at 510 nm with different metal ions (10 μM) at pH 7.4 in water.

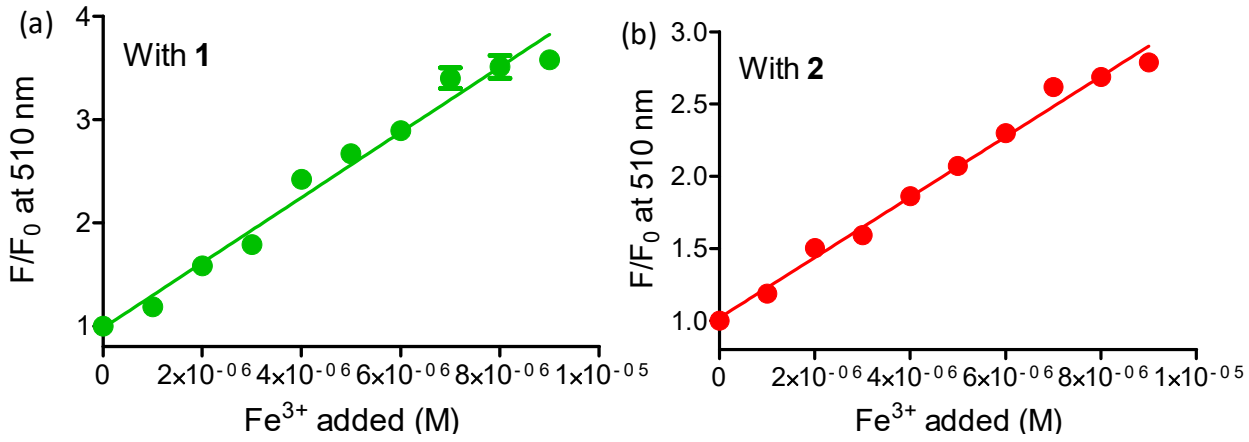

Figure S16. (a) Change in fluorescence of **1** (10 μM) at 510 nm upon addition of Fe^{3+} (0-11 μM) at pH 7.4 in water; (b) Change in fluorescence of **1** (10 μM) at 510 nm upon addition of Fe^{2+} (0-11 μM) at pH 7.4 in water

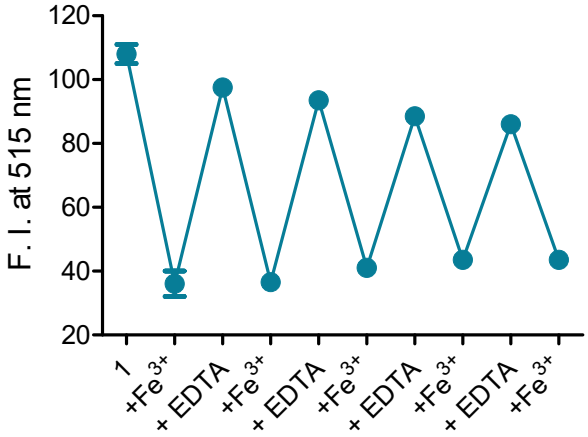

Figure S17. Change in fluorescence intensity of **1** (10 μM, λ_{ex} = 457 nm) at 510 nm upon sequential addition of Fe^{3+} (10 μM) and EDTA (10 μM) at pH 7.4 in water

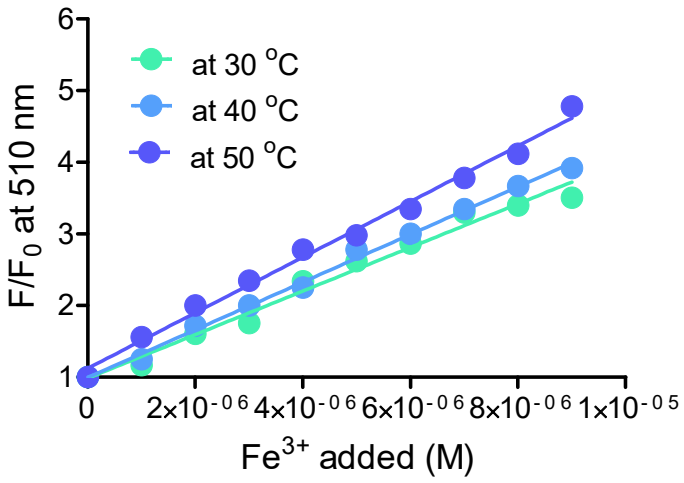

Temperature (°C)	Ksv (10^5 M^{-1})
30	3.02
40	3.35
50	4.08

Figure S17. Determination of Stern-Volmer quenching constant of **1** (10 μM, λ_{ex} = 457 nm) at 510 nm upon addition of Fe^{3+} (10 μM) at different temperature at pH 7.4 in water

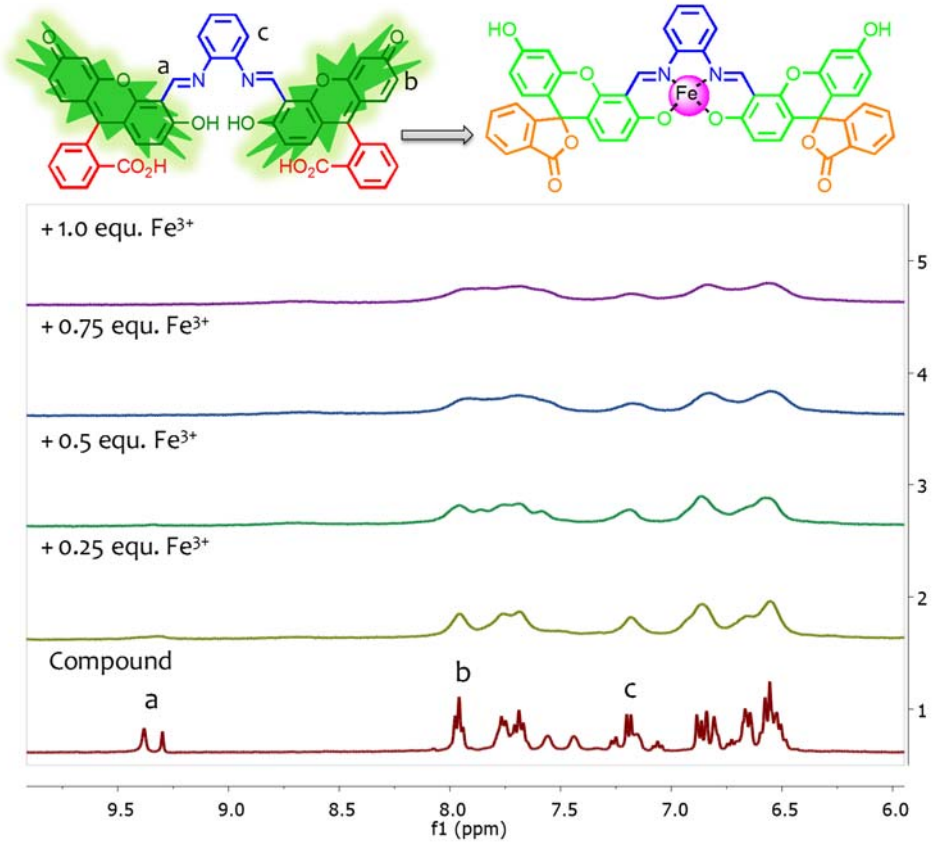

Figure S18. Partial ^{1}H-NMR spectra of **1** (5 mM) upon addition of Fe^{3+} (0-5 mM) DMSO-d_6/D_2O mixture (3:2) medium

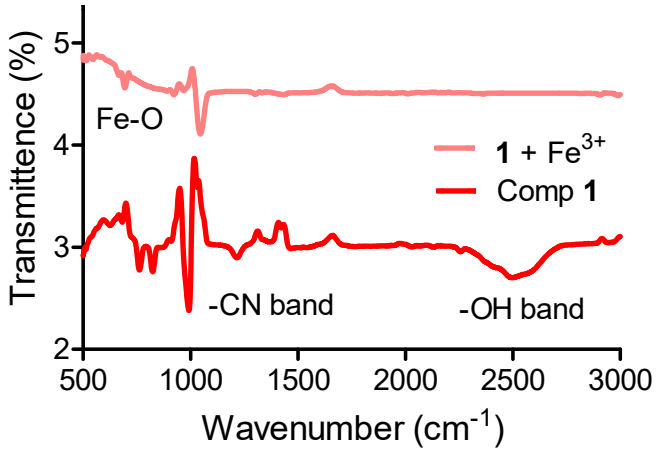

Figure S19. FT-IR spectra of **1** (0.5 mM) in presence of Fe^{3+} (0.5 mM) at pH 7.4 in water

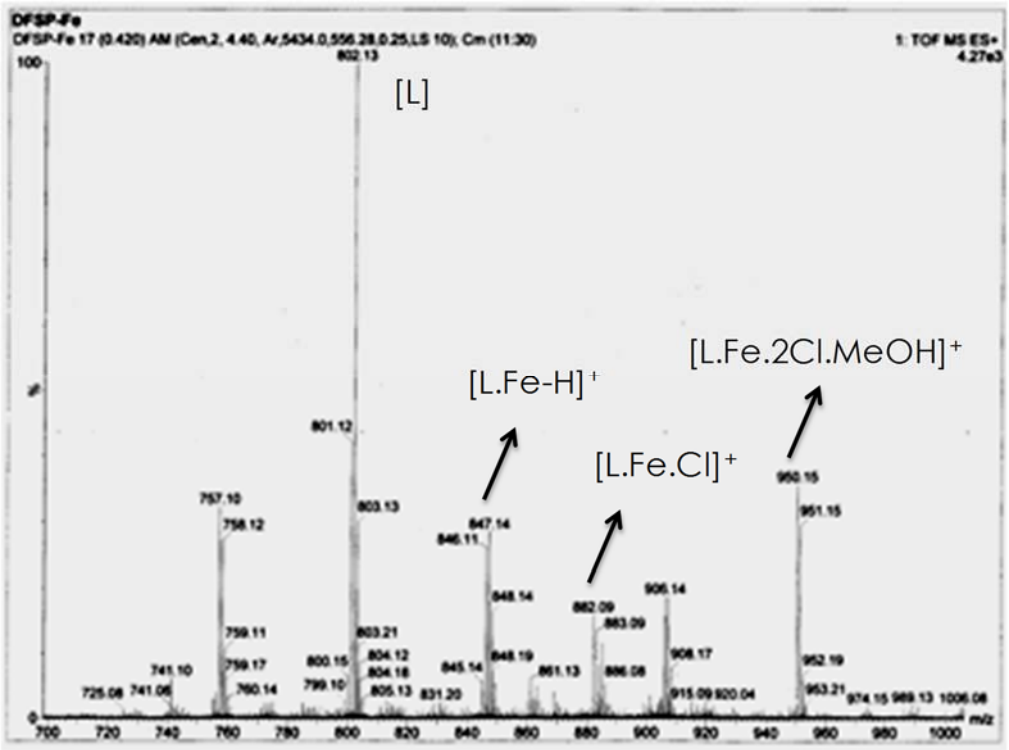

Figure S20. ESI-MS mass spectrum of **1** (0.5 mM) upon addition of Fe^{3+} (0.5 mM) at pH 7.4 in water

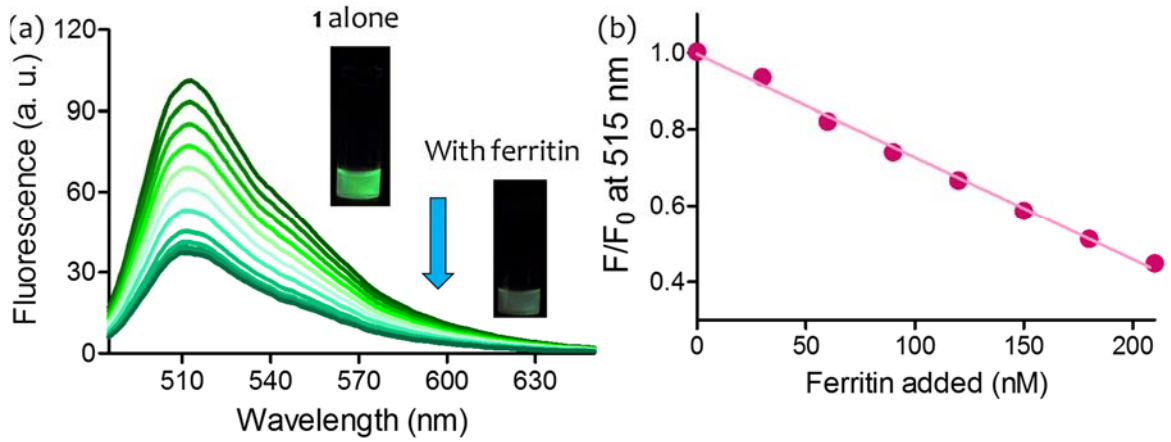

Figure S21. (a) Fluorescence titration of **1** (10 μM, λ_{ex} = 457 nm) with ferritin (0-300 nM) at pH 6.0 in water. (b) Change in emission intensity of **1** (10 μM, λ_{ex} = 457 nm) during titration with ferritin (0-220 nM)

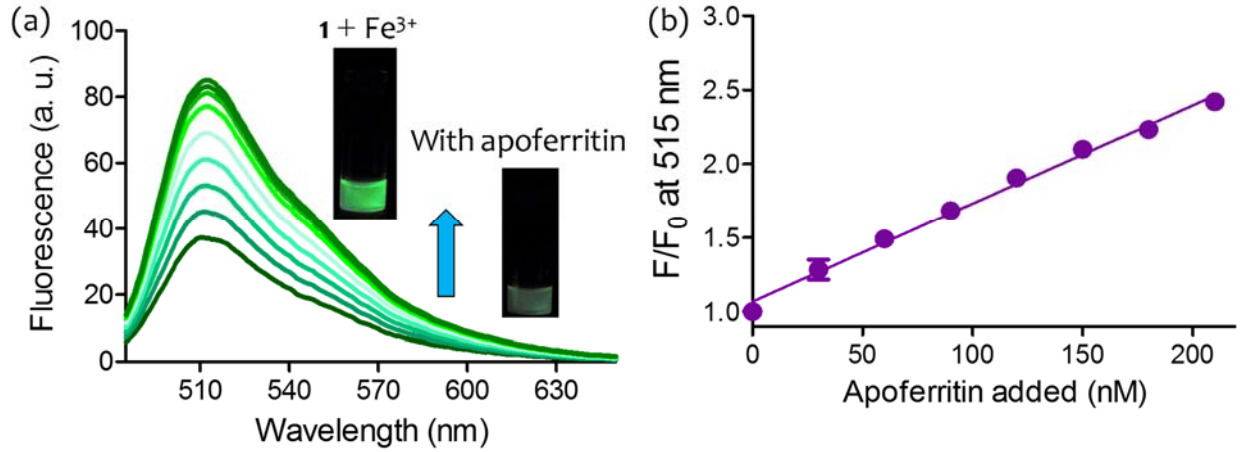

Figure S22. (a) Fluorescence titration of **1** + Fe^{3+} ([**1**] = 10 μM, [Fe^{3+}] = 10 μM, λ_{ex} = 457 nm) with apoferritin (0-300 nM) at pH 6.0 in water; (b) Change in emission intensity of **1** + Fe^{3+} ([**1**] = 10 μM, [Fe^{3+}] = 10 μM, λ_{ex} = 457 nm) during titration with apoferritin (0-220 nM) at pH 6.0 in water.

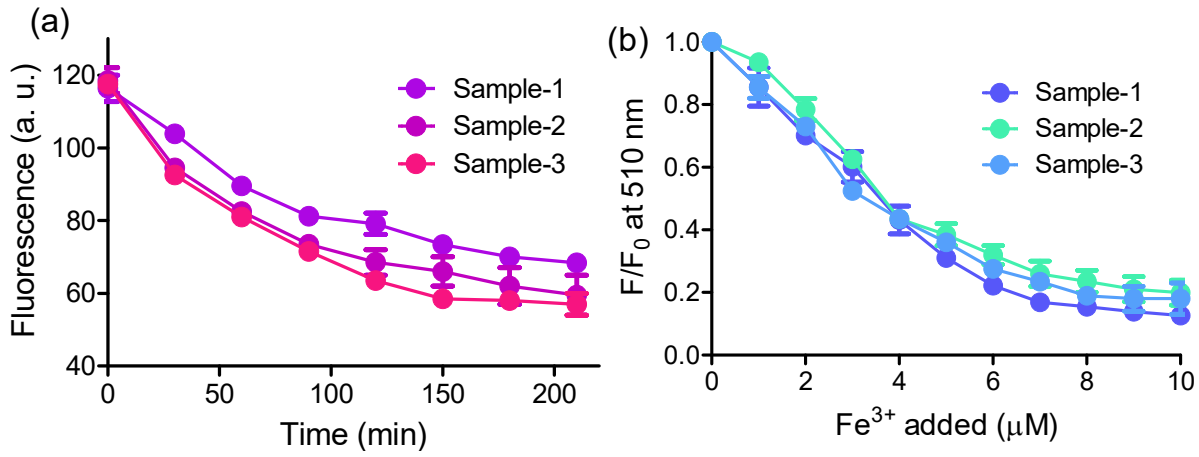

Figure S23. (a) Change in emission intensity of **1** (10 μM, λ_{ex} = 457 nm) at 515 nm with time (0-220 min) in blood serum samples (2.5/7.5 v/v with pH 7.4 buffer) at pH 4.5. (b) Change in emission intensity of **1** (10 μM, λ_{ex} = 457 nm) at 515 nm upon addition of Fe^{3+} in different blood serum samples (2.5/7.5 v/v with pH 7.4 buffer) at pH 7.4.

Blood serum samples	Serum Iron (μM) From present method	Average (μM)	% RSD	Fe^{3+} unbound (μM)	LIBC (μM) = Fe^{3+} added – Fe^{3+} unbound (Iron added: 20 μM)	TIBC (μM) = Serum Iron + Unbound Iron	Average (μM)	% RSD
Sample 1	3.65	3.64	1.65	6.77	13.23	16.88	16.83	0.58
	3.58			6.86	13.14	16.72		
	3.70			6.80	13.20	16.90		
Sample 2	4.25	4.20	1.04	6.41	13.59	17.84	17.84	0.09
	4.18			6.33	13.67	17.85		
	4.17			6.35	13.65	17.82		
Sample 3	4.62	4.60	0.55	5.82	14.18	18.80	18.83	0.19
	4.57			5.70	14.30	18.87		
	4.60			5.78	14.22	18.82		

Table S2. Estimation of Fe^{3+} in different diluted blood serum samples (2.5/7.5 v/v with pH 7.4 buffer) using compound **1** (10 μM, λ_{ex} = 457 nm) monitored at 515 nm.

Blood serum samples	Serum Iron In µg/dL (present method)	Serum Iron In µg/dL (AAS method)	% Error	TIBC In µg/dL (present method)	TIBC In µg/dL (AAS method)	% Error	Transferrin saturation (%) (present method)	Transferrin saturation (%) (AAS method)	% Error
Sample 1	61.15	62.50	2.39	282.80	285.28	1.16	21.6	21.9	1.37
	59.98			280.12					
	61.99			283.13					
Sample 2	71.20	72.58	3.15	298.88	308.34	3.19	23.6	23.5	0.43
	70.03			299.00					
	69.86			298.55					
Sample 3	77.04	78.15	1.61	314.97	320.12	1.45	24.3	24.4	0.40
	76.56			316.14					
	77.07			315.30					

Table S3. Determination of Diagnostic Parameters Associated with Serum Iron Estimation

(a)

Blood serum samples	Fe^{3+} Linear range (in µM)	Detection limit (in ppm)
Sample 1	0-6.3	0.052
Sample 2	0-5.4	0.045
Sample 3	0-6.0	0.038

(b)

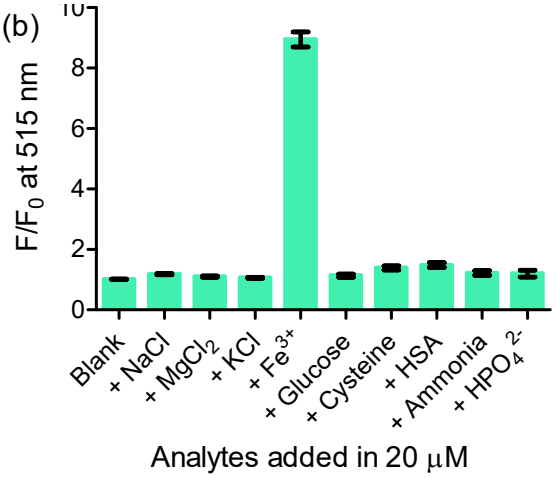

Figure S24. (a) Linear range as well as detection limit for Fe^{3+} sensing in different diluted blood serum samples (2.5/7.5 v/v with pH 7.4 buffer) using compound **1** (10 µM, λ_{ex} = 457 nm) monitored at 515 nm. (b) Change in emission intensity of 1 at 515 nm in presence of different analytes in diluted blood serum samples (2.5/7.5 v/v with pH 7.4 buffer).

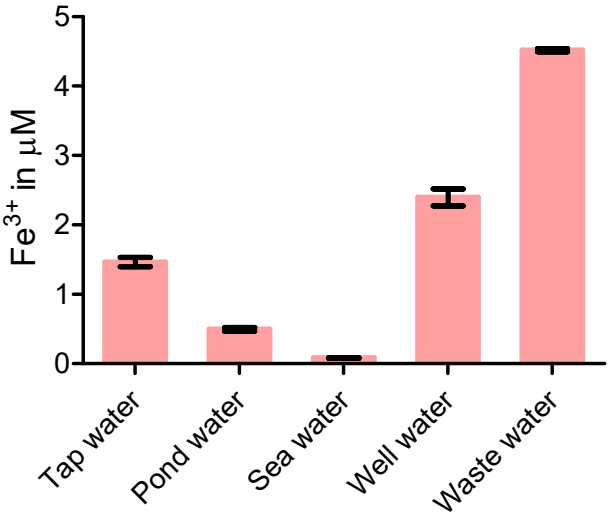

Figure S25. Estimation of Fe^{3+} (in µM) in different natural water samples using **1** (10 µM) at pH 7.4 in water.

Water Sources	Fe^{3+} level (n=3)	Fe^{3+} level (n=3)	(in % level)
	Proposed method In ppb	AAS method In ppb	Deviation
Tap	166.5 ± 5.2	170.2 ± 1.2	**2.9**
Pond	57.0 ± 1.5	52.4 ± 0.5	**9.5**
Sea	9.8 ± 0.5	8.5 ± 0.8	**15.2**
Well	247.2 ± 9.8	243.5 ± 2.5	**1.6**
Waste	488.4 ± 10.6	490.2 ± 4.2	**0.4**

Table S4. Estimation of Fe^{3+} (in µM) in different natural water samples using both present method as well as AAS method.

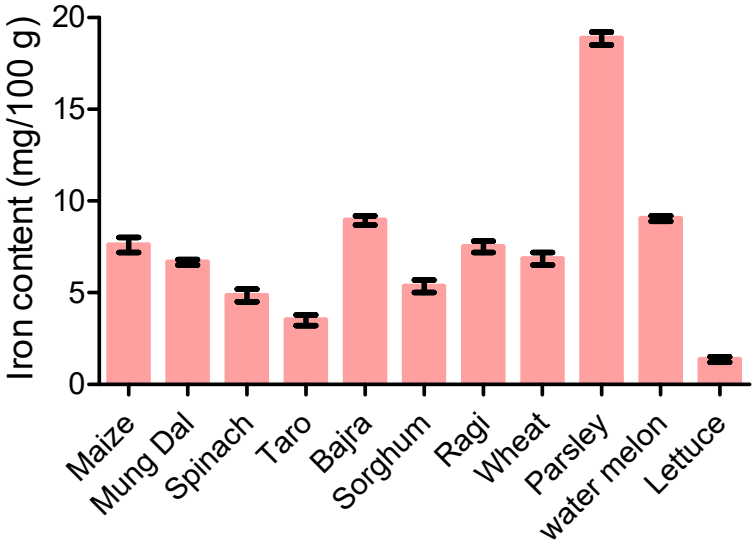

Figure S26. Estimation of iron (mg/100 g) in different agricultural samples using **1** (10 μM, λ_{ex} = 457 nm) at pH 7.4 in water

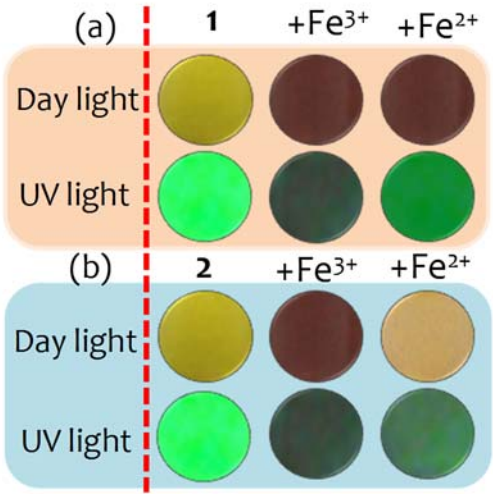

Figure S27. Compound coated color strips for discrimination of Fe^{3+} and Fe^{2+} using compounds **1** and **2.**

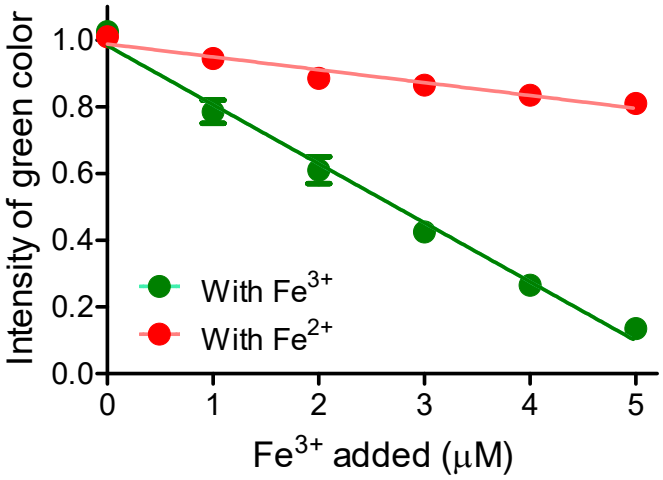

Figure S28. Compound coated color strips for discrimination of Fe^{3+} and Fe^{2+} using compounds **1.**

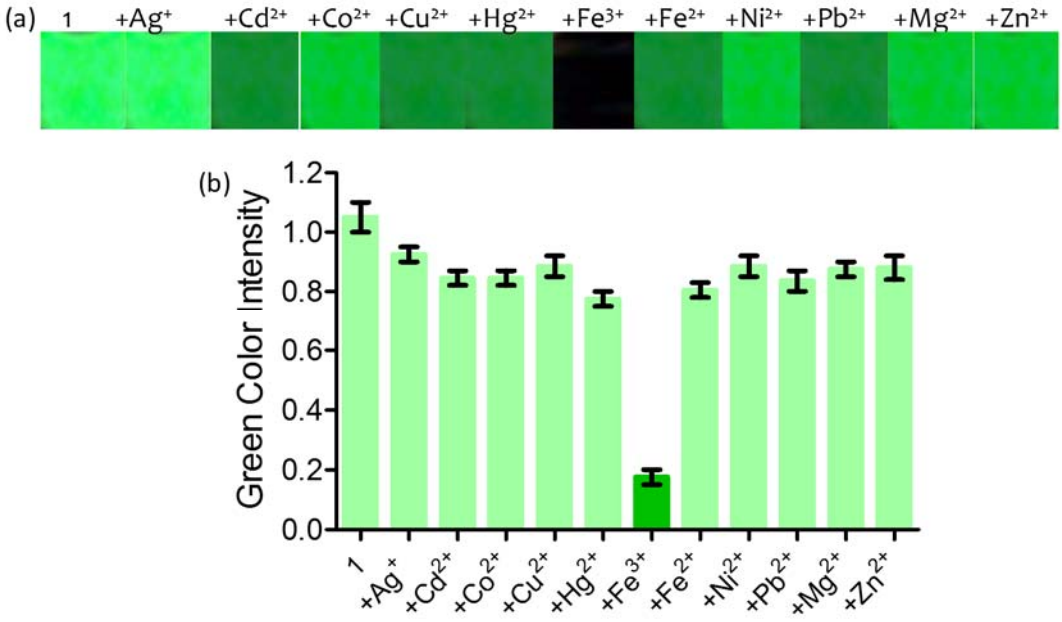

Figure S29. (a) Color strips for on-site detection of Fe^{3+}; selectivity was checked in presence of different metal ions. (b) Quantify the extent of emission change of color strips upon addition of different metal ions at pH 7.4 in water.

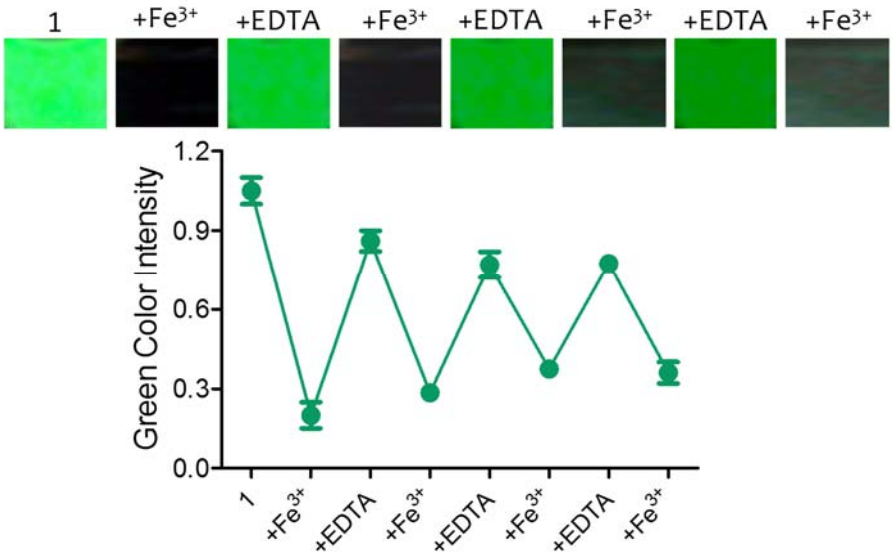

Figure S30. (a) Color strips for reversible detection of Fe^{3+}; equimolecular EDTA was used in each time. (b) Quantify the extent of emission change of color strips upon sequential addition of Fe^{3+} and EDTA.

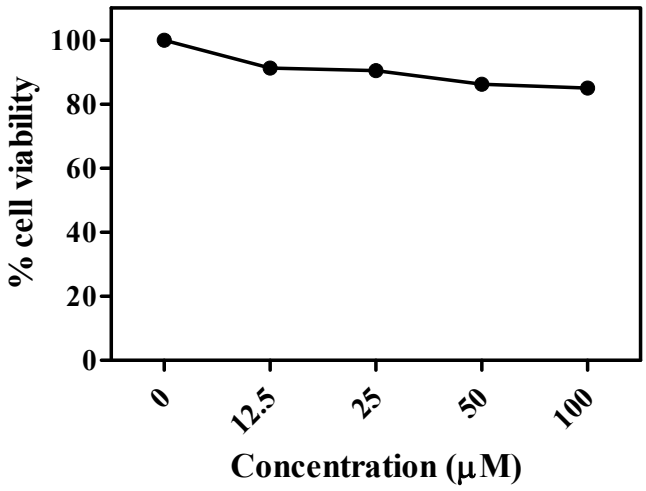

Figure S31. Plot of %cell viability against concentration of **1** in HeLa cells for 72 h treatment period.